JPIChE 52(2) 2024: 59-67

PAKISTAN INSTITUTE OF CHEMICAL ENGINEERS Since 1969

Journal of the Pakistan Institute of Chemical Engineers

Journal homepage: www.piche.org.pk/journals

DOI: https://doi.org/10.54693/piche.05227

Check for updates

Hydrodynamic and Thermal Analysis of Water Slugs in Super-Hydrophobic T-Junction Microchannel

M. Mohsin[1], H.M. Masood[1,2], Najaf Ali[1*], K. Shahzad[2], M. Hassan[1]

Submitted: 08/08/2024, Accepted: 10/04/2025, Published: 17/04/2025

Abstract

Microfluidics has garnered significant attention due to its vast potential and advancements in computational modeling. This study aims to examine air-water bubble flow behavior in a T-junction micro channel, emphasizing the role of slug flow, which is critical for applications such as micro reactors and micro channel heat sinks. A multiphase model was used to track the air-water interface and simulate slug production. A mesh independence study determined an optimal mesh size of 0.1mm, balancing accuracy and computational efficiency. A constant heat flux of 8850 W/m² was applied to the walls, and the resulting temperature variations were analyzed. Slug flow significantly enhanced heat transfer, resulting in a substantial reduction in wall temperature and an increase in the Nusselt number compared to single-phase flow. The heated wall exhibited temperature variations along its length due to the applied heat flux. Slug flow demonstrates superior heat transfer performance in micro channels compared to single-phase flow, indicating its potential for enhancing thermal management in microfluidic devices.

Keywords: Heat Transfer, Multi-Phase Flow, Bubble Flow, Micro-Channel, VOF (Volume of Fluid)

1. Introduction:

Microfluidics, the science and technology of manipulating fluids at the micro scale (typically 10^{-9} to 10^{-6} meters), has emerged as a disruptive technology across diverse fields. The ability to integrate multiple unit processes onto a single chip has led to the development of "Lab-on-a-Chip" (LOC) devices, offering significant advantages, including portability, reduced reagent consumption, and faster analysis times [1]. LOC devices can be designed for user-friendly operation, requiring minimal expertise, which is particularly valuable for point-of-care diagnostics and applications in resource-limited settings. The small size of these devices also enhances their portability, facilitating on-site analysis and field applications. Microfluidics has found extensive applications in various fields. In diagnostics, LOC devices are revolutionizing the detection of various analytes, enabling rapid, sensitive, and specific point-of-care testing and eliminating the need for centralized laboratory facilities [1]. Microfluidics also holds promise for improving the efficiency and economics of carbon capture technologies through reduced reagent volumes and enhanced mass transfer. In biological and medical research, microfluidic systems provide unprecedented control over the cellular microenvironment, allowing for precise studies of cell behavior, drug responses, and physiological processes. For instance, the ability to observe live cell responses to micro-level drug injections is a powerful tool in drug discovery and personalized medicine [2]. Furthermore, microfluidic devices are being explored for targeted drug delivery, offering the potential to improve drug efficacy, reduce side effects, and minimize patient discomfort by precisely controlling

[1]Department of Chemical Engineering, NFC Institute of Engineering and Fertilizer Research, Faisalabad, Pakistan

[2]Institute of Chemical Engineering & Technology, University of the Punjab, Lahore, Pakistan

***Corresponding author:** Najaf Ali (najafawan@hotmail.com)

drug delivery to specific locations [5].

Beyond these applications, microfluidic nozzles have played a crucial role in the development of inkjet printing technology, replacing earlier, less efficient methods and demonstrating the technology's broad impact [6, 7, 8, 9, 10, 11].Many of these chemical and biological processes involve multiphase flows, where two or more fluid phases (e.g., gas-liquid, liquid-liquid) interact within micro channels. Understanding the behavior of these multiphase flows at the micro scale is critical for the design and optimization of microfluidic devices. However, the behavior of these flows is complex, governed by factors such as surface tension, viscosity, interfacial forces, and channel geometry, leading to phenomena not observed at the macro scale. Despite its importance, certain aspects of multiphase flow in micro channels remain under-explored. Specifically, the current numerical work on water droplet formation in continuous air flow through water-repellent micro channels has not been thoroughly studied, according to a rigorous examination of recent literature. Additionally, the augmentation of heat transfer caused by slugs running with air bubbles dispersed in continuous water, and vice versa, has also received little research [12, 13, 14, 15].This study aims to address these gaps by employing a reliable Computational Fluid Dynamics (CFD) model to investigate gas-liquid multiphase flows in a microfluidic T-junction. CFD offers a powerful tool to simulate fluid dynamics by solving the governing equations of fluid mechanics, such as the Navier-Stokes equations, using numerical methods. The Volume of Fluid (VOF) method, a widely used interface-tracking technique in CFD, will be employed to accurately capture the interface between the gas and liquid phases. This method is well-suited for simulating multiphase flows with large interfacial deformations, as it can effectively handle the complex flow patterns encountered in micro channels. The simulations will be performed using a computational mesh with sufficient resolution and refinement to ensure the accuracy and stability of the results. The specific details of the CFD model and simulation setup, including boundary conditions and solution procedures, will be described in detail. This approach will provide valuable insights into the fundamental mechanisms governing water droplet formation and heat transfer enhancement in micro channel multiphase flows. Mesh independence analysis is a crucial step in any Computational Fluid Dynamics (CFD) study, including the one on microfluidics, to ensure that the numerical results are reliable and not dependent on the size of the computational mesh. Here's a detailed explanation in the context of the article: Why Mesh Independence Analysis Is Important Discretization: In CFD, the physical domain of the problem (e.g., the micro channel) is divided into a large number of small elements or cells, forming the "mesh." The governing equations of fluid flow, heat transfer, and mass transfer are then solved numerically within these cells. Accuracy vs. Computational Cost: A finer mesh (more cells) generally leads to more accurate results because it better resolves the spatial variations of the flow variables. However, a finer mesh also requires significantly more computational resources (memory and time).Mesh Dependence: If the mesh is too coarse, the numerical solution may be inaccurate, and the results may change significantly if the mesh size is changed. This is called "mesh dependence. “Mesh Independence: The goal of mesh independence analysis is to find a mesh that is fine enough to produce accurate results but not so fine that it requires excessive computational resources. At this point, the solution is considered "mesh independent. “How Mesh Independence Analysis Was Likely Performed in the Article Based on the abstract, here's how the researchers likely performed mesh independence analysis: Initial Mesh: They started with a relatively coarse mesh for the micro channel geometry. Simulation: They ran the CFD simulation with this mesh and obtained the results for the variables of interest (e.g., temperature, velocity, pressure). Mesh Refinement: They then refined the mesh by increasing the number of cells. This could involve: Reducing the size of the cells uniformly throughout the domain. Reducing the size of the cells in specific regions where the flow gradients are high (e.g., near the walls, at the T-junction, or in the regions where bubbles or droplets are present).Simulation with Refined Mesh: They ran the CFD simulation again with the refined mesh and obtained new results. Comparison of Results: They compared the results from the coarse mesh and the refined mesh. Iteration: They repeated steps 3-5, further refining the mesh, until the changes in the results between successive mesh refinements became sufficiently small. Mesh Independence: The mesh was considered "mesh independent" when further refinement produced negligible changes in the results.

Optimal Mesh Size: The abstract mentions that a mesh size of 0.1mm was determined to be optimal. This means that varied the mesh size around this value and found that it provided a good balance between accuracy and computational cost. What Variables to Monitor for Mesh Independence In the context of this microfluidics study, the researchers likely monitored the following variables to assess mesh independence: Temperature: Since the study focuses on heat transfer, they would have monitored the temperature distribution along the walls of the micro channel, particularly the maximum wall temperature and the average wall temperature. Nusselt Number: The Nusselt number is a dimensionless quantity that characterizes the effectiveness of heat transfer. They would have monitored the change in the Nusselt number with mesh refinement. Flow Field Variables: They might have also monitored the velocity profiles, pressure distribution, and the shape and size of the bubbles or droplets to ensure that these were not significantly affected by the mesh size. Conclusion: from the Abstract the abstract states that "A rigorous mesh independence analysis was conducted to determine the optimal mesh size (0.1mm) for accuracy and computational efficiency." This indicates that the researchers took the necessary steps to ensure the reliability of their CFD simulations and that the results presented in the article are not significantly affected by the mesh resolution. Key aspects of experimental investigations into slug flow, as conducted by Walsh et al. and other researchers, typically include: These experiments often involve horizontal pipes, where controlled flows of gas (typically air) and liquid (often water) are introduced. The pipe dimensions (diameter and length) are critical parameters. Instrumentation is crucial for accurate measurements. Measurement Techniques are Electrical Capacitance Tomography (ECT) is frequently used to visualize and quantify the flow patterns within the pipe. ECT allows researchers to determine parameters such as: Parameters Investigated are Superficial gas and liquid velocities, Slug frequency, Slug length and Taylor bubble length, Void fraction, Pressure gradients.

The studies investigate the relationship between flow parameters and slug characteristics. It was often analyzed the stochastic nature of slug flow, highlighting the variability of slug lengths and frequencies. The data obtained are used to validate empirical correlations and develop mechanistic models of slug flow. To investigate the flow behavior (hydrodynamics) of water slugs within a super hydrophobic T-junction micro channel. To analyze the heat transfer characteristics (thermal analysis) of these water slugs within the same micro channel. To understand how the super hydrophobic properties of the microchannel influence both the fluid flow and heat transfer processes.

2. Materials and Methods:

2.1. Meshing and Geometric Specs:

The technique of the mesh independence analysis has been thoroughly detailed in the methodology section above. Simulations were ran for multiple mesh sizes at a gas flow rate of 30 ml/min and a liquid flow rate of 1.5 ml/min, using the mesh independence study methodology, and got diverse findings. Various mesh sizes observed until the results for the parameter of interest, which in present instance was slug length, started to converge. The liquid phase volume fraction contour generated from numerical simulation. The relationship between numerical slug length and mesh size, as well as the error between numerical and experimental slug length for various mesh sizes. In Table (1) properties of materials are given. After reviewing the findings of the mesh independent study, it was clear that a mesh size of 0.1mm would become an excellent decision. As a result, the mesh size of 0.1mm will be employed for validation and analytics throughout this project. Figure 1 has shown the schematic diagram in which gas is the continuous phase and liquid is the dispersed phase[16].

Table 1: Properties of Materials [16]

Material	Properties		
$m3$	Density ($\frac{kg}{}$)	Viscosity (m.S)	Surface Tension ($\frac{N}{m}$)
Water	998.2	1.002×10^{-3}	0.07288
Air	1.205	1.808×10^{-5}	

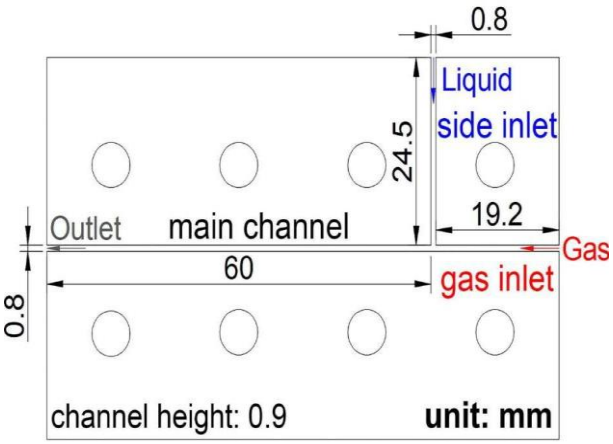

Figure 1: Schematic of experimental setup [16]

2.2. Mathematical Model Description:

As previously stated, VOF (Fluid Volume) is best suited for bubbly and slug flows, and it is based on following the interface across the domain using the volume fraction value of each cell. Each whenever a phase is added to the system, a new variable is introduced [17], [18]. It is the volume fraction value that is used to assign the values of the variables and characteristics to every cell within the domain. If two phases are immiscible and also not interpenetrating, as in present instance, the total of mass fraction of phase in each computing cell equals unity. VOF model owes its simplicity and convenience to the fact that only one set of equations of continuity, momentum and energy, common to both phases, is solved[19], [20].

The equations of continuity, momentum and energy are following:

$$\frac{1}{\rho_p}\cdot\frac{\partial(\rho\,\alpha_p)}{\partial t}\cdots\alpha_p\rho\,v\,)=S_{\alpha_p}+\sum_{q=1}^{n}(\dot{m}_{qp}-\dot{m}_{pq}) \quad (1)$$

Where P_p is the density $\dot{m}_{qp}$ is mass transfer rate from phase q to phase 'p' while $\dot{m}_{pq}$ is the rate of mass transfer from phase 'p' to phase q. And $S_{\alpha p}$ is the source term which can be zero or non-zero depending upon the conditions.

The equation for momentum is given as below:

$$\frac{\partial(\rho\vec{v})}{\partial t}+\nabla.(\rho\vec{v}\vec{v})=-\nabla p+\nabla.[\mu(\nabla\vec{v}+\nabla\vec{v}^{T})]+\rho\vec{g}+\vec{F} \quad (1)$$

$\frac{\vec{F}}{\partial t}$ is the Source term, ∇p is pressure term, $\frac{(\rho\vec{v})}{+}$ $\nabla.(\rho\vec{v}\vec{v})$ are transient and convective terms respectively and $\nabla.[(\nabla\vec{v}+\nabla\vec{v}^{T})]$ is the viscous term.

And the energy equation is following:

$$\frac{\partial(\rho E)}{\partial t}+\nabla.(\vec{v}(\rho E+p))=\nabla.(k_{eff}\nabla T)+S_h \quad (2)$$

2.3. Numerical Solution:

The production of water bubbles in air passing thru a microchannel was simulated using ANSYS FLUENT R18.2.For pressure interpolation, the Pressure Staggering Option was employed, and the Pressure Implicit using Splitting of Operators (PISO) method was used to produce pressure-velocity coupling. The second-order upwind discretization approach was used to solve the momentum transport equation. And he geometric reconstruction interpolation approach was used to trace the interface. Under- relaxation factors were chosen to 0.7, 1 and 1 for momentum, density, & body forces iterative solutions, respectively. In Figure 2, it could be seen that how slug formation observed in ANSYS fluid.

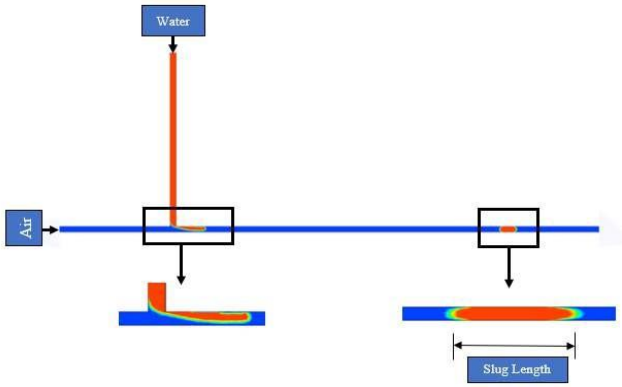

Figure 2: Slug formation contours

1. Results and Discussion:

3.1. Hydrodynamic Analysis:

The hydrodynamic analysis of the numerical model was conducted to ensure its fidelity in replicating the experimental setup. A crucial step in this process was validation against a benchmark study, specifically the experimental work of Song et al. (2019). This validation was performed by comparing the simulated slug generation time and slug length with the experimental data. The comparison revealed a strong agreement between the numerical simulations and the experimental results, confirming the model's accuracy.

As depicted in Figure 3, the slug length exhibited a positive correlation with mesh size, indicating the importance of mesh resolution in capturing the flow dynamics accurately. However, discrepancies between the experimental and numerical slug lengths were observed, particularly at lower gas flow rates. This suggests that the numerical model's accuracy is sensitive to gas flow rate, with higher flow rates yielding better agreement.

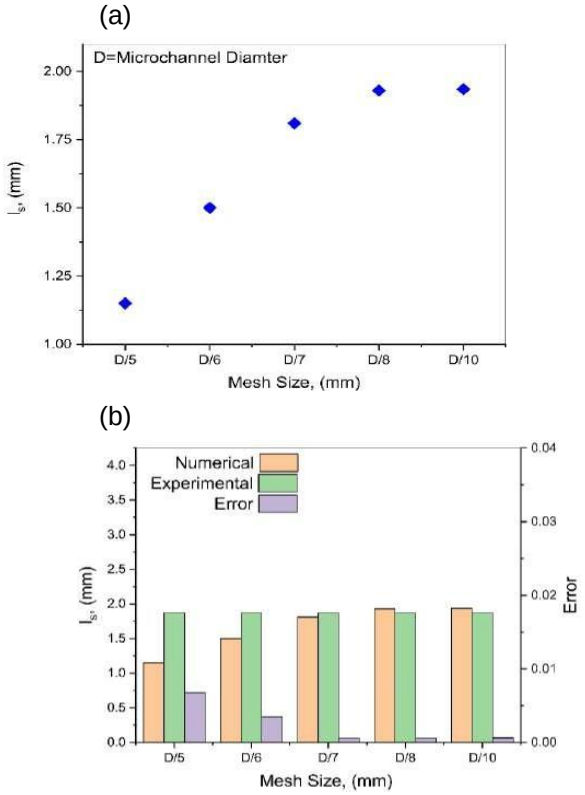

Figure 3: (a) Mesh Study (b) Comparison

The observed increase in error at lower gas flow rates can be attributed to the increased influence of surface tension and viscous forces, which are often challenging to model accurately in numerical simulations (Ghanem et al., 2016).The positive correlation between mesh size and slug length highlights the necessity of a sufficiently refined mesh to resolve the intricate flow patterns associated with slug flow (Cubaud & Ho-Yung, 2004).

Figure 4 demonstrates the inverse relationship between gas flow rate and slug length. As the gas flow rate increases, the slug length decreases. This is consistent with the principle that higher gas flow rates lead to increased shear stress and momentum transfer, resulting in the formation of shorter slugs. Conversely, Figure 5 illustrates a direct correlation between liquid flow rate and slug length. Increased liquid flow rate enhances the momentum of liquid phase, which results in the formation of longer slugs.

The inverse relationship between gas flow rate and slug length aligns with observations reported by Thulasidas et al. (1995), who demonstrated the influence of gas velocity on slug formation and length. The effect of liquid flow rate on slug length is consistent with the findings of Triplett et al. (1999) that show that increasing liquid flow rate increases the slug length.

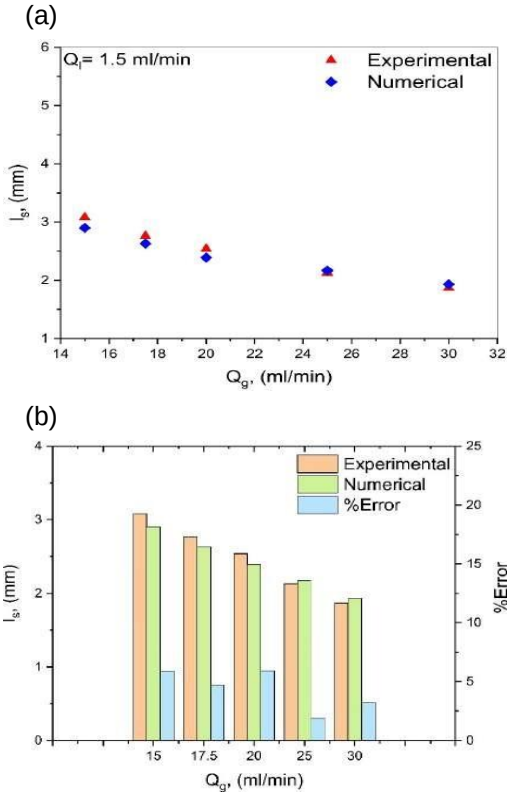

Figure 4: Slug length vs Gas flow rate

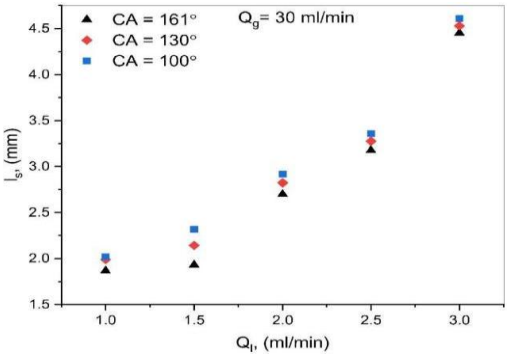

Figure 5: Slug length variation with liquid flow rate

3.2. Heat Transfer Analysis:

The heat transfer analysis involved comparing the simulated results of slug flow with air scatter and slug flow with water scatter against experimental data from Walsh et al.'s work. The simulations aimed to determine

the wall temperature and Nusselt number profiles under varying flow conditions.

The simulated wall temperature profile for slug flow with air scatter showed good agreement with the experimental data. As depicted in Figure 6, the wall temperature increased with distance from the thermal entry. However, fluctuations in the temperature profile were observed, attributed to the periodic passage of water slugs, which have a high thermal capacitance and conductivity.

The temperature drop observed during water slug passage is due to the combined effects of high thermal capacitance, thermal conductivity, and internal recirculation within the water slugs.

The overall heat transfer enhancement in slug flow with air scatter was found to be limited, primarily due to the dominance of air, which has a low thermal mass. The entrance region showed maximum wall temperature due to the absence of the thermal boundary layer. As the boundary layer develops, the wall temperature decreases.

Figure 7 compares the wall temperature profile for slug flow with water scatter to that of single-phase water flow. The slug flow exhibited significantly lower wall temperatures, indicating enhanced heat transfer. This enhancement is attributed to the increased velocity of water slugs and the internal recirculation caused by the presence of air bubbles. Figure 7 also illustrates the Nusselt number profile, which decreased with increasing distance from the entrance region. This indicates a reduction in the heat transfer coefficient as the thermal boundary layer develops. The oscillations in the Nusselt number profile were less pronounced compared to slug flow with air scatter, due to the higher thermal capacitance of water. Figure 8 showed the increase of wall temperature with the increase of distance. Figure 9 shows that smaller slug lengths result in higher Nusselt numbers, which is consistent with the enhanced heat transfer associated with increased interfacial area and mixing. Figure 10 summarizes the comparison of all analyzed cases, showing that the air-dispersed case exhibits the highest Nusselt number, indicating the most effective heat transfer. The enhancement of heat transfer in slug flow due to internal recirculation and increased velocity has been extensively studied (Kreutzer et al., 2005). The observation that smaller slug sizes lead to higher Nusselt numbers is consistent with the findings of Kashid and Agarwaal (2007) that heat transfer rate increases with the decrease of slug length

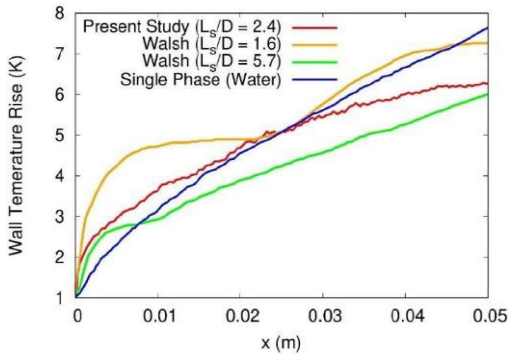

Figure 6: Validation of present study with [8] for wall temp. rise

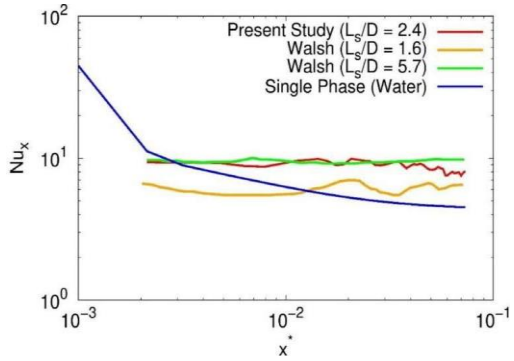

Figure 7: Validation of present study with [8] for Nu no

The increased heat transfer was owing to the fact that water slugs have internal recirculation, as well as high thermal capacity and conductivity. The effect of internal recirculation and some other parameters increases as more water slugs pass.

It's also worth noting that oscillations have begun, but with a smaller amplitude than in a bubble flow with water scattered, due to the thermal properties of water being significantly greater than those of air and it generates a considerable dip in wall temperature rise everywhere it passes, however in the case of air scattered in water, many bubbles flow through the channel followed by water slugs, and the temperature increase fluctuation was not as noticeable as it was in the case of air dispersed in air. Figure 8 showed that with rise the of distance boundary layer formed and wall temperature rises with the respect of different phases.

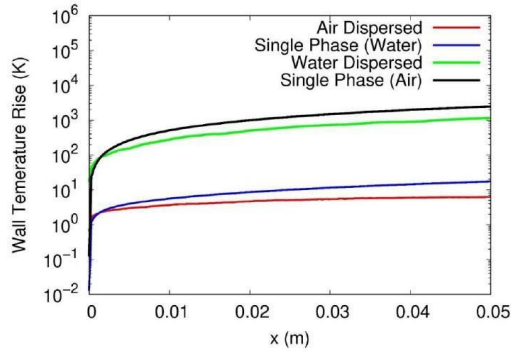

Figure 8: Wall Temperature Rise vs Distance

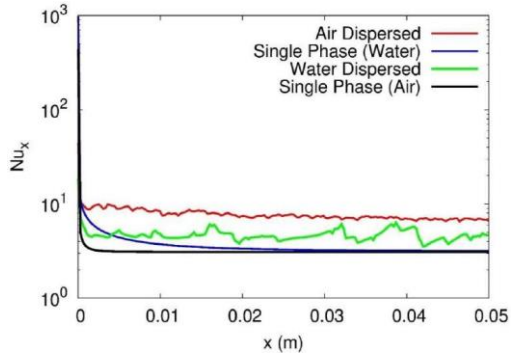

Figure 9: Nusselt number vs distance

The Nusselt numbers for L s/D=1.6 and L s/D=2.4 are very differs at first, but the difference becomes apparent later, and the Nusselt number for L s/D=1.6 was noticeably higher than that for L s/D=2.4, which were consistent with the above-mentioned fact that smaller slug size gives rise to lesser wall temperature rise and thus more heat transfer enhancement, i.e. Nusselt number enhancement as shown in the figure 9. It's also worth noting that, much as in the case of a spik in wall temperature, In the beginning, there were no heat conduction enhancement, but once the slug has travelled one slug length, the slug flow has begun to have an effect on the heat transfer enhancement. After comparing of all cases it was observed that air dispersed case best fit because in this case Nusselt number obtained maximum, when Nusselt number obtained higher heat transfer coefficient also high as shown in figure 10. Because once the slug has travelled one slug length, the recirculation process begins.

5. Conclusion

This study meticulously examined the production and behavior of water bubbles within a micro channel featuring a T-junction, employing numerical simulations validated against experimental data from Song et al. Initially, a mesh independence study was conducted to ensure the accuracy and efficiency of the simulations. The hydrodynamic analysis revealed a strong correlation between the numerical model and experimental results, confirming the model's reliability. Notably, slug length was observed to increase with water phase flow rate at a constant air flow rate, while it decreased with increasing air phase flow rate. Furthermore, the study highlighted the significant influence of contact angle, demonstrating an inverse relationship with slug length. The thermal analysis then explored the heat transfer characteristics of slug flow within the micro channel's heated segment. Intriguingly, slug flow was found to degrade heat transfer in the entry regions where a thermal boundary layer formed, contrasting with the superior performance of air-dispersed bubble flow, which exhibited the maximum heat transfer enhancement. This enhancement is attributed to the increased mixing and interfacial surface area provided by the air bubbles within the liquid slugs. Conversely, single-phase air flow displayed the lowest heat transfer values, and slug flow with water dispersion yielded only weak heat transfer enhancement, likely due to the low thermal mass of the continuous air phase. These findings underscore the critical role of flow parameters and phase distribution in both the hydrodynamic and thermal behavior of slug flow in micro channels, offering valuable insights for the design and optimization of microfluidic systems.

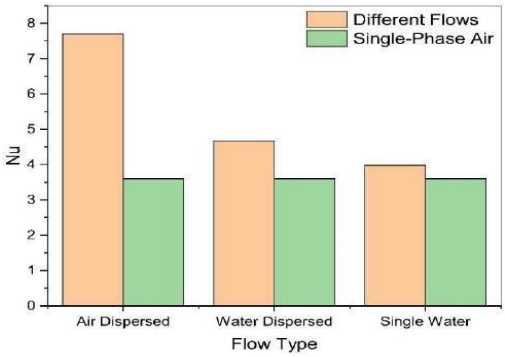

Figure 10: Comparison of average Nu no. for different cases in relation with single phase airflow

References

[1] L. Dai, W. Cai, and F. Xin, "Numerical study on bubble formation of a gases liquid flow in a T-junction microchannel," *Chemical*

Engineering & Technology: Industrial Chemistry Plant Equipment Process Engineering•Biotechnology, vol. 32, pp. 1984-1991, 2009.

[2] D. MB and D. R, "Aerosol drug delivery: developments in device design and clinical use," *Lancet (London, England)*, vol. 377, no. 9770, pp. 1032–1045, 2011, doi: 10.1016/S0140-6736(10)60926-9.

[3] W. J. Duncanson, T. Lin, A. R. Abate, S. Seiffert, R. K. Shah, and D. A. Weitz, "Microfluidic synthesis of advanced microparticles for encapsulation and controlled release," *Lab Chip*, vol. 12, no. 12, pp. 2135–2145, May 2012, doi: 10.1039/C2LC21164E.

[4] C. H. Ahn *et al.*, "Disposable smart lab on a chip for point-of-care clinical diagnostics," *Proc. IEEE*, vol. 92, no. 1, pp. 154–173, 2004, doi: 10.1109/JPROC.2003.820548.

[5] P. Cui and S. Wang, "Application of microfluidic chip technology in pharmaceutical analysis: A review," *J. Pharm. Anal.*, vol. 9, no. 4, pp. 238–247, Aug. 2019, doi: 10.1016 /J. JPHA. 2018.12.001.

[6] K. Jiang, A. X. Lu, P. Dimitrakopoulos, D. L. DeVoe, and S. R. Raghavan, "Microfluidic generation of uniform water droplets using gas as the continuous phase," *J. Colloid Interface Sci.*, vol. 448, pp. 275–279, Jun. 2015, doi: 10.1016/J.JCIS.2015.02.023.

[7] B. Bhushan, *Handbook technology (Air Liquide)*. 2019.

[8] C. D. Ahrberg, A. Manz, and B. G. Chung, "Polymerase chain reaction in microfluidic devices,"*Lab Chip*, vol. 16, no. 20, pp. 3866–3884, Oct. 2016, doi: 10.1039/C6LC00984K.

[9] P. A. Walsh, E. J. Walsh, and Y. S. Muzychka, "Heat transfer model for gas-liquid slug flows under constant flux," *Int. J. Heat Mass Transf.*, vol. 53, no. 15–16, pp. 3193–3201, 2010, doi: 10.1016/j.ijheatmasstransfer.2010.03.007.

[10] D. B. Tuckerman and R. F. W. Pease, "High-Performance Heat Sinking for VLSI," *IEEE Electron Device Lett.*, vol. EDL-2, no. 5, pp. 126–129, 1981, doi: 10.1109/EDL.1981.25367.

[11] W. Pan *et al.*, "Device-scale CFD modeling of gas-liquid multiphase flow and amine absorption for CO2 capture," *Greenh. Gases Sci. Technol.*, vol. 8, no. 3, pp. 603–620, 2018, doi: 10.1002/ghg.1770.

[12] Y. Song, F. Xin, and Y. Xu, "Catalytic exchange of hydrogen isotopes intensified by two-phase stratified flow in wettability designable micro channels," *Lab Chip*, vol. 20, no. 12, pp. 2154–2165, 2020, doi: 10.1039/d0lc00250j.

[13] X. C. i Solvas and A. deMello, "Droplet microfluidics: recent developments and future applications," *Chem. Commun.*, vol. 47, no. 7, pp. 1936–1942, Feb. 2011, doi: 10.1039/C0CC02474K.

[14] A. Mehdizadeh, S. A. Sherif, and W. E. Lear, "Numerical simulation of thermofluid characteristics of two-phase slug flow in micro channels," *Int. J. Heat Mass Transf.*, vol. 54, no. 15–16, pp. 3457– 3465, 2011, doi: 10.1016/j.ijheatmasstransfer.2011.03.040.

[15] R. M. Santos and M. Kawaji, "Gas-liquid slug formation at a rectangular microchannel t-junction: A CFD benchmark case," *Cent. Eur. J. Eng.*, vol. 1, no. 4, pp. 341–360, 2011, doi: 10.2478/s13531-011-0038-1.

[16] T. Bandara, N. T. Nguyen, and G. Rosengarten, "Slug flow heat transfer without phase change in micro channels: A review," *Chem. Eng. Sci.*, vol. 126, pp. 283–295, 2015, doi: 10.1016/j.ces.2014.12.007.

[17] Y. Song, F. Xin, G. Guangyong, S. Lou, C. Cao, and J. Wang, "Uniform generation of water slugs in air flowing through superhydrophobic micro channels with T-junction," *Chem. Eng. Sci.*, vol. 199, pp. 439–450, 2019, doi: 10.1016/j.ces.2019.01.041.

[18] M.J. Cheah, I.G. Kevrekidis and J.B. Benziger, "Water Slug Formation and Motion in Gas Flow

Channels: The Effects of Geometry, Surface Wettability, And Gravity," *Langmuir*, vol. 29, no. 31, pp. 9918–9934, Aug. 2013, doi: 10.1021/LA4011967.

[19] M. Mastiani, B. Mosavati, and M. Kim, "Numerical simulation of high inertial liquid-in-gas droplet in a T-junction microchannel," *RSC Adv.*, vol. 7, no. 77, pp. 48512–48525, 2017, doi: 10.1039/c7ra09710g.

[20] "ANSYS FLUENT 12.0 Theory Guide - 16. Multiphase Flows." https://www.afs.enea.it/project/ neptunius/ docs/ fluent /html/ th /node288.htm (accessed Mar. 28, 2021).

[21] R. Gupta, D.F. Fletcher, and B.S. Haynes, "On the CFD modelling of Taylor flow in micro channels," *Chem. Eng. Sci.*, vol. 64, no. 12, pp. 2941–2950, Jun. 2009, doi: 10.1016/J.CES.2009.03.01